

Contents lists available at ScienceDirect

Mechanical Systems and Signal Processing

journal homepage: www.elsevier.com/locate/ymssp



Design of a networking stress wave communication method along pipelines

Sihong He^{a,1}, Guangmin Zhang^{a,b,1}, Gangbing Song^{a,*}

- ^a Department of Mechanical Engineering, University of Houston, Houston, TX 77204, USA
- ^b School of Electrical Engineering and Intelligentization, Dongguan University of Technology, Dongguan 523808, China

ARTICLE INFO

Keywords:

Stress wave communication Networking sensor communication Orthogonal variable spreading factor (OVSF) Piezoelectric transducer

ABSTRACT

Stress waves are increasingly employed in structural health monitoring (SHM) systems of pipelines based on sensor networks. Data transmission among sensors is crucial for the overall stress waves based SHM system. Since conventional communications are hampered by limited transmission ranges when in some environments, such as in soil and water, it is essential to develop an alternative approach to deal with the issues. This paper proposes a stress wave communication networking method that can be implemented among multiple sensors. The proposed work introduces Orthogonal Variable Spreading Factor (OVSF) codes to achieve multiple-access stress wave channels by using piezoelectric transducers. In this paper, both frequency-domain and time-domain channel responses are estimated, and communication schemes are thereby designed to achieve data transmission among multiple sensors based on the features of multiple channels. The experiments are conducted on a T-shape pipeline structure in the laboratory environment, and the results verify the feasibility of the method. Experimental results show that the data rate of each single channel reaches 250 bps.

1. Introduction

Recent years have seen the rapid development of structural health monitoring (SHM) system that uses embedded sensor and advanced algorithms along with communication capacity to monitor structural health status in real-time [1]. Stress waves play an important role in SHM to monitor structural integrity and to detect structural damages [2–4]. For pipeline implementations, the stress wave based SHM system includes transmitters and sensors that are permanently mounted on the pipelines of interest [5,6], and investigations have found that stress waves perform well in detecting diverse damages on pipeline structures [7], including corrosion [8,9], leakage [10], crack [11,12], and impact [13]. Often, Lead Zirconate Titanate (PZT), a type of piezoelectric material with strong piezoelectric effect, is used as a transmitter to generate and as a sensor to detect stress waves [14,15]. Furthermore, PZTs have fast responses and wide bandwidth [16], and PZTs can be fabricated into transducers with different sizes and shapes for various structures [17,18], including pipelines [19]. Stress waves excited by PZT transmitters can propagate a long distance along the pipelines [20,21],

It is noteworthy that data transmission among sensors is a crucial aspect in the stress wave based SHM systems, especially sensor networks where sensors are integrated to monitor and detect larger pipeline ranges with better performances and efficiency. The information needs to be delivered to a center processing unit from downstream sensors. Necessary reactions and explicit messages will

E-mail address: gsong@uh.edu (G. Song).

https://doi.org/10.1016/j.ymssp.2021.108192

Received 9 June 2020; Received in revised form 5 May 2021; Accepted 25 June 2021

^{*} Corresponding author.

 $^{^{1}}$ The co-first-author due to their equal contributions with the first author.

then be sent back to intended receivers. Data transmission lays the foundation for normal operation of SHM sensor networks.

Data transmission among SHM sensors generally adopts conventional communication technologies such as wired communications and radio frequency (RF) communications. Information-conveying signals are modulated and delivered by carrier waves through cables (in wired communication systems) or air (in RF communication systems). However, conventional communications are proved to be inappropriate in some circumstances. For instance, it is expensive and time-consuming to install and regularly maintain cables for broad stress wave based SHM sensor networks on underground or underwater pipelines. Electromagnetic waves, namely the carrier wave in RF communications, attenuate exponentially in water and soil, thus its transmission range is limited. Therefore, it is essential to develop an alternative data transmission method for SHM sensor networks of inaccessible pipelines, such as buried pipelines and offshore pipelines.

Stress wave communication (SWC) is an emerging data transmission method [22–24]. Unlike traditional communications that use electromagnetic waves, the stress waves are utilized to carry information coded signals and the propagation medium is the solid wave guide. As stress waves can travel a long distance through wave guide media in aquatic and underground environments [25], the hurdles that hinder the use of conventional RF communications are of no issues for SWC. Furthermore, SWC can use the currently existing transducers of stress wave based SHM systems to launch or receive information bearing stress waves. Through appropriate deployment of sensors, it is promising to achieve data transmission among sensors that serve in the original SHM system. Thereby, there is no need to install additional cables or communication device as it does with conventional communication methods. Researches of stress wave communication are mainly devoted in achievements of through-wall communications and logging while drilling (LWD) data transmission. Regarding through-wall communications, stress waves enable data transmission through a thick metal barrier [26–30], where it is undesirable to drill holes for cable installation, such as pressure vessels and watertight metal bulkheads. Through-wall stress waves communication systems couple an external transducer and an internal transducer with the conducting medium (the metal wall) to transfer information. In the LWD applications, a drill string sets up the communication channel to transport stress waves from the bottom of the borehole to the ground surface. Stress wave data transmission greatly improves the data rate compared to what can be achieved using conventional mud-pulse telemetry [31,32].

Explorations of the SWC applications on pipelines have received much attention in recent years [33]. Jin et al. [34–36] employed time reversal technique in the stress wave communication on a metal pipe to prevent elongated waveforms caused by dispersion. In their papers, a received pulse waveform is reversed and utilized to modulate signals with pulse position modulation (PPM), and the transmitted signals present good data transmission performances. Huang et al. [37] adopted Amplitude Shift Keying (ASK) to modulate signals and accomplished data transmission on a metal pipe using an Electro Magnetic Acoustic Transducer (EMAT) to emit stress waves. And a Chirp-On-Off Keying (Chirp-OOK) based stress wave communication was developed by Chakraborty et al. [38,39] Their method helps to combat the frequency selectivity of the communication channel. Experiments were conducted on a 4.8-meter metal pipe both in air and water, and the results stated the achievement of data rate up to 100 bps. Joseph et al. [40] utilized Amplitude Modulation (AM) in stress wave communication and demonstrated the SWC system successfully on a water-filled pipe and the data rate reached 100 bps. The achievements indicate that it is feasible to apply stress wave communication through pipelines with a variety of methods. Nevertheless, the researches on pipeline stress wave communication are mainly focused on Single-Input-Single-Output (SISO) systems, that is, only one transmitter and one receiver are considered. In many situations, a networked sensor-actuator system is needed when multiple sensors and actuators are involved.

This paper proposes a novel method to achieve stress wave data transmission among networking sensors on pipelines, which is an extension of SISO stress wave communication. Channel estimation is conducted both in frequency and time domains to clarify the features of each stress wave channel. Orthogonal Variable Spreading Factor (OVSF) codes are employed in this paper for multiple-access channels due to the orthogonality between codes. Each node in the sensor network is assigned a unique local OVSF code. Transmitting signals are coded with the local OVSF codes and modulated with Binary Phase Shift Keying (BPSK), and the demodulated signals at the receiver's end can be decoded by the local OVSF codes. Schemes for Single-Input-Multiple-Output (SIMO) and Multiple-Input-Single-Output data transmission are designed differently based on the channel features. For SIMO data transmission, the center unit launches multiple signals for different receivers simultaneously by Code Division Multiple Access (CDMA) scheme so that high efficiency can be obtained. On the other hand, Time-Division Multiple Access (TDMA) scheme is used for Multiple-Input-Single-Output (MISO) data transmission to simplify the post processing procedure. Therefore, preamble signals are designed in the TDMA scheme to synchronize and identify signals from distinct sensors.

To the authors' best knowledge, the method proposed in this paper is the first reported instance that applies stress waves as communication carriers into the data transmission of networking sensors. It is demonstrated that the method is feasible by experiments conducted on a T-shape structure welded by 2 pipeline components. Experimental results demonstrate that signals can be successfully transferred and interpreted using the designed schemes and the data rate can reach 250 bps. The rest of this paper is organized as follows. Section 2 presents associated theoretical background, which introduces basic principles for the proposed networking stress wave communication design. Section 3 follows to explain the design of the proposed method. The experiment and results discussion are illustrated in Section 4. Conclusions and future works wind up in Section 5.

2. Theoretical background of networking stress wave communications

Studies on the characteristics of stress wave traveling along pipelines reveal that the propagation modes can be classified into three families: longitudinal modes (L), transverse modes (T), and flexural modes (F). Multiple modes are inevitably involved along with the propagation when applying an asymmetric stress wave excitation method. Additionally, there are tremendous possible propagation paths between two random points on a pipeline. Consequently, when traveling with multimode and multipath effects along pipelines,

stress wave signals undergo distortion and dispersion, by which the signals are decreased and temporally extended. Therefore, this paper explores different channel access methods in the proposed networking stress wave communication in order to ensure satisfactory performances with severely distorted and dispersed signals. When performing single-input-multiple-output (SIMO) data transmission, synchronous code division multiple access (CDMA) is employed since the transmitting signals experience identically in SIMO channels, where the orthogonality among multiple users' codes is well exploited. On the other hand, as severe signal distortion and dispersion make it much more difficult to apply channel equalization to SW communications than that in conventional RF communications, time-division multiple access (TDMA) is utilized in multiple-input–single-output (MISO) communication so as to prevent complex channel equalization and signal superimposition. The related principles and implementations of the proposed networking stress wave communication method are elaborated as follows.

2.1. Channel response

Channel response analysis is a crucial aspect for communication scheme design and the follow-up simulations. In this paper, we employ the power spectral density (PSD) of acquired signals to estimate the channel response in frequency domain, which specifies available bandwidth for stress wave communication over multiple channels. Moreover, a 1-D version of 'CLEAN' algorithm [41–43] is utilized to provide time-domain channel estimation.

2.1.1. PSD channel estimation

The power spectral density refers to the measure of signal's power in terms of frequency. With the aid of Fast Fourier Transform (FFT) algorithm at discrete frequencies, the PSD of the measured input signal x[n] is defined as the auto-spectrum by [44]

$$\widehat{S}_{XX}(f) = X^{*}(f)X(f) = \frac{1}{T} \left| \sum_{n=1}^{N} x[n]e^{-j2\pi f n\Delta t} \right|^{2}$$
(1)

where the data length of x[n] is N and the corresponding record length $T = N\Delta t$. X(f) is FFT of the input signal x[n] and $X^*(f)$ is the complex conjugate of X(f).

Accordingly, the measured cross-spectrum from the input signal x[n] to the output signal y[n] is defined as

$$\widehat{S}_{XY}(f) = X^*(f)Y(f) \tag{2}$$

Since the relation between measured input and output signals can be described as

$$y[n] = h[n] *x[n] + w[n]$$
 (3)

where h[n] represents the impulse response of the channel and w[n] is the noise. Thereby,

$$Y(f) = H(f)X(f) + W(f)$$
(4)

$$\widehat{S}_{XY}(f) = H(f)\widehat{S}_{XX}(f) + \widehat{S}_{XW}(f) \tag{5}$$

$$H(f) = \frac{\widehat{S}_{XY}(f) - \widehat{S}_{XW}(f)}{\widehat{S}_{XX}(f)} \tag{6}$$

2.1.2. Time-domain channel measurement

The time-domain characterization of propagation channels depicts the comprehensive multimode and multipath effects on signals. In particular, the impulse response implies the arriving time delays of signals from all multipath components. Thereby, time-domain channel response may influence the design of stress wave communication schemes. In this paper, CLEAN algorithm is applied to extract impulse responses of the communication channels.

The CLEAN algorithm iteratively searches the received signal for the most significant component with templates and subtracts it and then continues on searching for the second component [45]. The channel model is defined as

$$h(t) = \sum_{k} a_k \delta(t - \tau_k) \tag{7}$$

where a_k and τ_k respectively specify the amplitude and time delay of the kth component under the comprehensive effect of multimode and multipath. a_k and τ_k are both derived and recorded through the CLEAN loop, by which the autocorrelation of its template and the cross-correlation between the template and the received signal are iteratively adopted.

2.2. OVSF code

When a single transmitter in the SWC system is in use to deliver stress wave signals to multiple receivers, synchronous CDMA is employed to allow the transmitter to send information simultaneously over multiple channels. CDMA utilizes spread spectrum technology, where signals are spread over a broad spectrum before transmitted, in order to ensure there is no undue interference

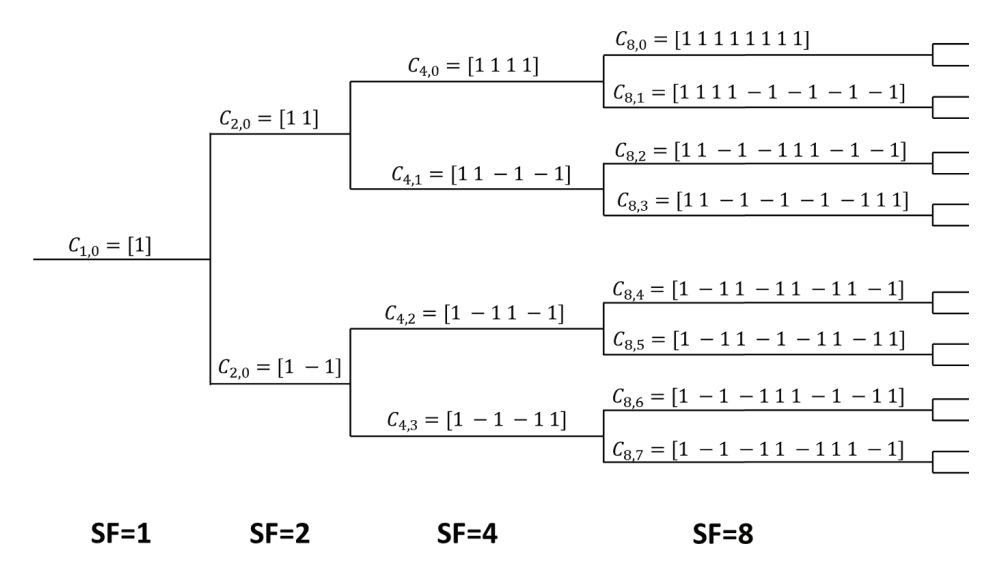


Fig. 1. Tree construction of OVSF codes.

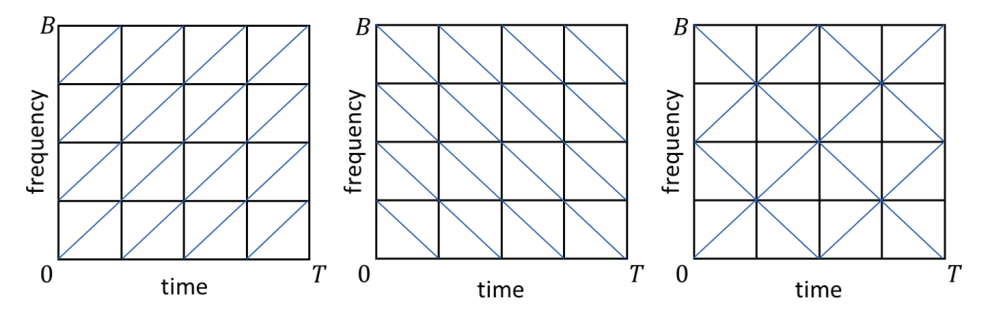


Fig. 2. Illustration of OFDM chirp bases.

between signals. As an implementation of CDMA, Orthogonal Variable Spreading Factor (OVSF) was initially introduced for the channelization of 3G communication systems. OVSF codes are defined recursively by an OVSF code tree (Fig. 1.) and they preserve mutual orthogonality between each other. In the SIMO stress wave communication system, each receiver is assigned a unique OVSF code, thereby signals for the intended receiver can be decoded using the exclusive local code.

The codes in the tree satisfy the following properties [46]:

a. Denote $C_{q,m} = [C_{q,m}(0), C_{q,m}(1), \cdots, C_{q,m}(q-1)]$ and $C_{q,k} = [C_{q,k}(0), C_{q,k}(1), \cdots, C_{q,k}(q-1)]$ as any two codes from the same layer q. Then,

$$P_{C_{q,m}C_{q,k}} = \sum_{i=0}^{q-1} C_{q,m}(i)C_{q,k}(i) = \begin{cases} 0, m \neq k \\ q, m = k. \end{cases}$$
(8)

b. Denote $C_{q,m} = [C_{q,m}(0), C_{q,m}(1), \cdots, C_{q,m}(q-1)]$ and $C_{p,k} = [C_{q,k}(0), C_{q,k}(1), \cdots, C_{q,k}(p-1)]$ as any two codes from two different layers q and p. And the lengths of the two codes are respectively N_q and N_p . Here we assume p > q for convenience. Then $C_{q,m}$ and $C_{p,k}$ are orthogonal to each other except that one is the successor of the other one.

2.3. The design of preamble signals in TDMA

As different channels reduce and elongate SW signals to varying extents, it is complicated and consuming to separate information waveforms from different transmitters if they are superimposed. Therefore, TDMA is exploited in MISO data transmission to divide time into fractions, and signals from different transmitters are processing successively in time segments. In order to synchronize signals and distinguish the sender of transmitted signals, preamble signals are indispensable for each transmitter. In this paper, autocorrelation is utilized on the preamble signals to detect time delays, so it is important to ensure good correlation property of the preamble signals for good detection performance. One of the technologies in MIMO radar system, the orthogonal frequency division multiplexing (OFDM) chirp signal [47,48], is introduced in this paper for preamble signal design since it can meet the requirements of correlation property gracefully. OFDM chirp signals are designed based on conventional chirp signals. It contains multiple sub-chirps of varying carrier frequencies. In this paper, all preamble signals are designed based on the following three OFDM chirp bases, namely, the upchirp basis, the down-chirp basis, and the hybrid-chirp basis, as shown in Fig. 2. Different preamble waveforms are thereby obtained by diversifying the bases.

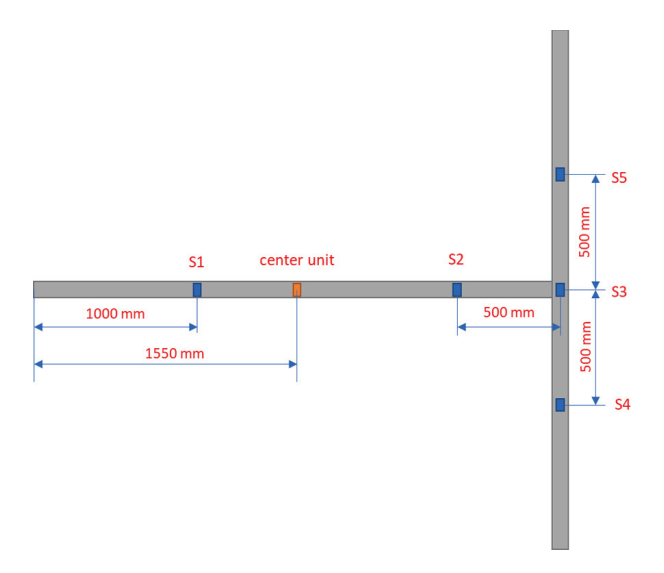


Fig. 3. Illustration of the T-shape pipeline.

Then, a general OFDM chirp basis with M temporal sub-chirps and N subcarriers can be hence defined as

$$s(t) = \sum_{m=0}^{M-1} \sum_{n=0}^{N-1} u(t - mT_b) exp \left[j2\pi \left(f_{m,n}(t - mT_b) + k_{m,n}(t - mT_b)^2 / 2 \right) \right]$$
(9)

where T_b is the duration of one sub-chirp, and u(t) = 1 for $0 \le t \le T_b$. Thus, the total duration of the OFDM chirp signal can be found by $T = MT_b$. Denote B_b as the subcarrier bandwidth and the total available bandwidth of the signal is $B = NB_b$. Then, $f_{m,n}$ and $k_{m,n}$ respectively defines the starting frequency and chirp rate of the mth duration at the nth subcarrier.

The OFDM bases are modulated with random matrices to create waveform diversity between each other. Denote a random matrix as

$$R = [r_1, r_2, \cdots, r_M]$$

where r_m is an integer and $1 \le r_m \le N$ for $m = 1, 2, \dots, M$. The integer r_m defines that the r_m th subcarrier in the mth sub-chirp is selected to create the preamble, and other subcarriers in the same sub-chirp are filtered out. Thus, the preamble signal can be then presented by

$$p(t) = \sum_{m=0}^{M-1} u(t - mT_b) exp \left[j2\pi \left(f_{m,r_m} (t - mT_b) + k_{m,r_m} (t - mT_b)^2 / 2 \right) \right]$$
(10)

Assume $p_a(t)$ and $p_b(t)$ are the preamble signals of the *ath* transmitter and the bth transmitter, and they are respectively generated with random matrices $R = [r_1, r_2, \cdots, r_m]$ and $W = [w_1, w_2, \cdots, w_m]$. $h_a(t)$ and $h_b(t)$ define the corresponding channel impulse responses from the transmitter to the intended receiver. Then, the received signals are given as

$$r_a(t) = p_a(t) * h_a(t) + n_a(t)$$
 (11)

$$r_b(t) = p_b(t) * h_b(t) + n_b(t)$$
 (12)

where $n_a(t)$ and $n_b(t)$ are noises obtained from respective channels.

Then, the autocorrelation and cross-correlation functions used to time the received signals are defined as

$$C_{aa}(t) = r_a(t) * p_a(-t) = [p_a(t) * h_a(t) + n_a(t)] * p_a(-t) = [p_a(t) * p_a(-t)] * h_a(t) + n_a(t) * p_a(-t)$$
(13)

$$C_{ab}(t) = r_a(t) * p_b(-t) = [p_a(t) * h_a(t) + n_a(t)] * p_b(-t) = [p_a(t) * p_b(-t)] * h_a(t) + n_a(t) * p_b(-t)$$

$$(14)$$

$$C_{bb}(t) = r_b(t) * p_b(-t) = [p_b(t) * h_b(t) + n_b(t)] * p_b(-t) = [p_b(t) * p_b(-t)] * h_b(t) + n_b(t) * p_b(-t)$$
(15)

$$C_{ba}(t) = r_b(t) * p_a(-t) = [p_b(t) * h_b(t) + n_b(t)] * p_a(-t) = [p_b(t) * p_a(-t)] * h_b(t) + n_b(t) * p_a(-t)$$
(16)

Only when the peak of autocorrelation functions is prominently higher than that of cross-correlation functions, can the received signals be correctly synchronized. As noises are relatively low compared to the received signals, the second term in Eqs. (13–16) can be neglected. Therefore, the essential goal of designing the preamble signals, which enables the received signals to be synchronized by correlating with the transmitted one, is to create high autocorrelation and suppress cross-correlation interferences under the effect of multipath and multimode channels. By observing Eq. (10), the preamble signals differentiate from others by using different subcarriers

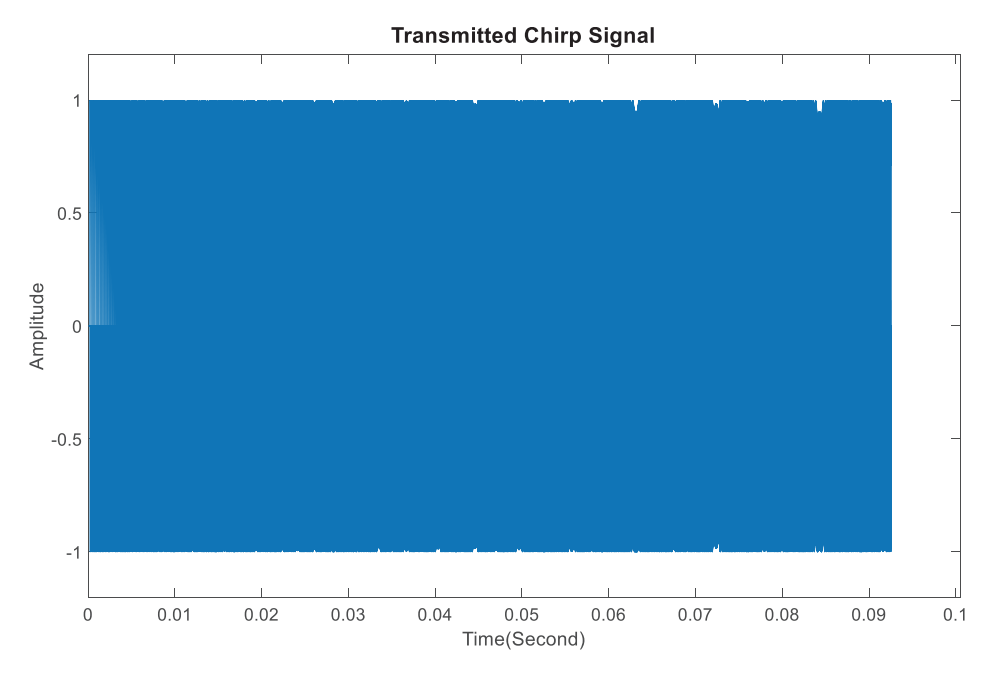


Fig. 4. Transmitted Chirp Signal.

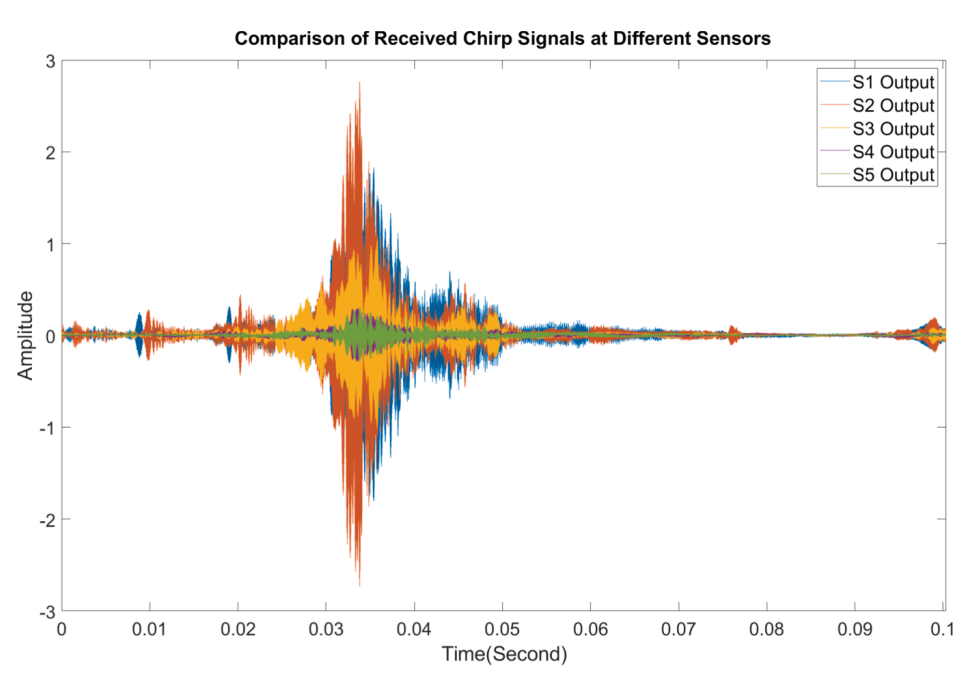


Fig. 5. Comparison of Received Chirp Signals at Different Sensors.

in one duration. Therefore, multiple preamble signals can be designed by diversifying the random matrices used to generate the signals, that is, diversifying the starting frequencies and chirp rates of the subcarriers. Moreover, it is an effective way to suppress cross-correlation interferences by adopting different carrier durations.

3. Networking stress wave communication design and implementation

As mentioned in Section 2, different schemes are applied to achieve the stress wave SIMO and MISO transmission systems respectively. This section first describes the results of channel estimation both in frequency domain and time domain using the methods as aforementioned. The available bandwidth is clearly presented via channel estimation, which is crucial for the overall communication system design. Then, preamble signals are designed to synchronize and specify signals from distinct transmitters in the MISO system. Correlation analysis of the simulated received preamble signals is illustrated. The following explains the overall networking stress wave communication system design.

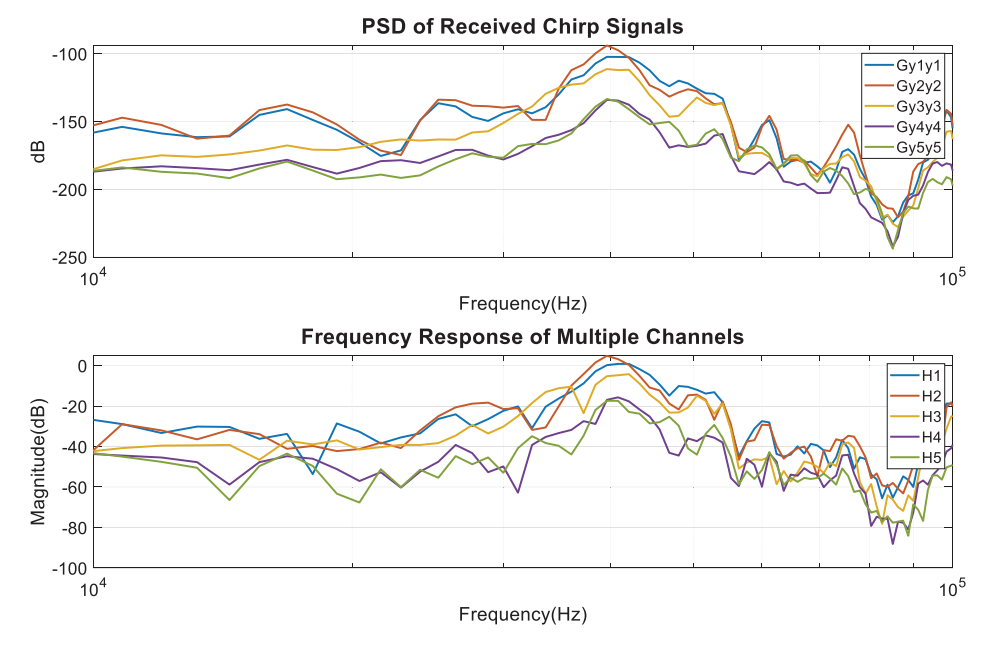


Fig. 6. Illustration of Channel Responses.

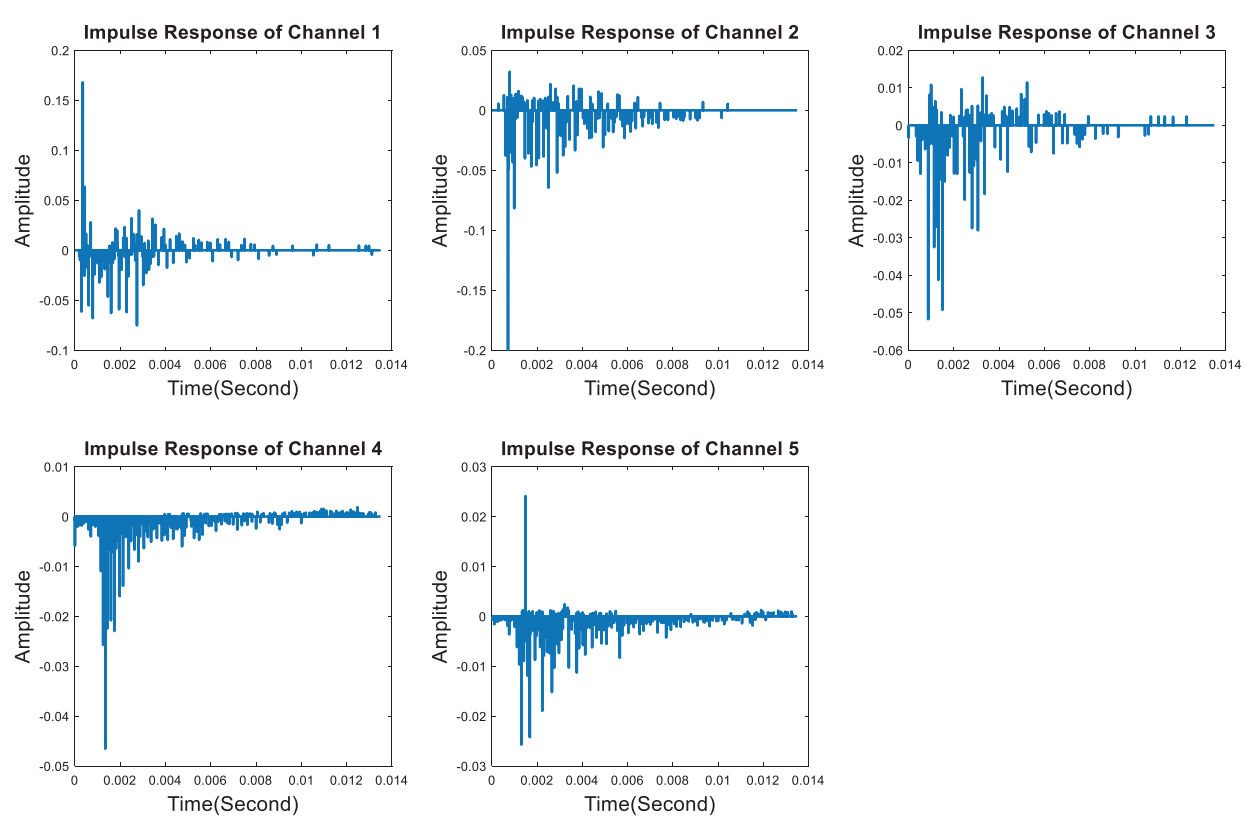


Fig. 7. Impulse response of the channels.

3.1. Results and analysis of channel estimation

The channel estimation is performed on a T-shape pipeline structure as shown in Fig. 3. Two galvanized steel pipes ($53.8 \times 50.8 \times 3048$ mm) are welded together, and piezoelectric transducers are distributed on the pipeline in the presented configuration. The transducer marked in blue serves as the center unit, where signals from the other transducers are collected in MISO data transmission and information is launched in SIMO data transmission. Channels estimated in the follows are constructed by the center unit, the propagation media and the corresponding receivers.

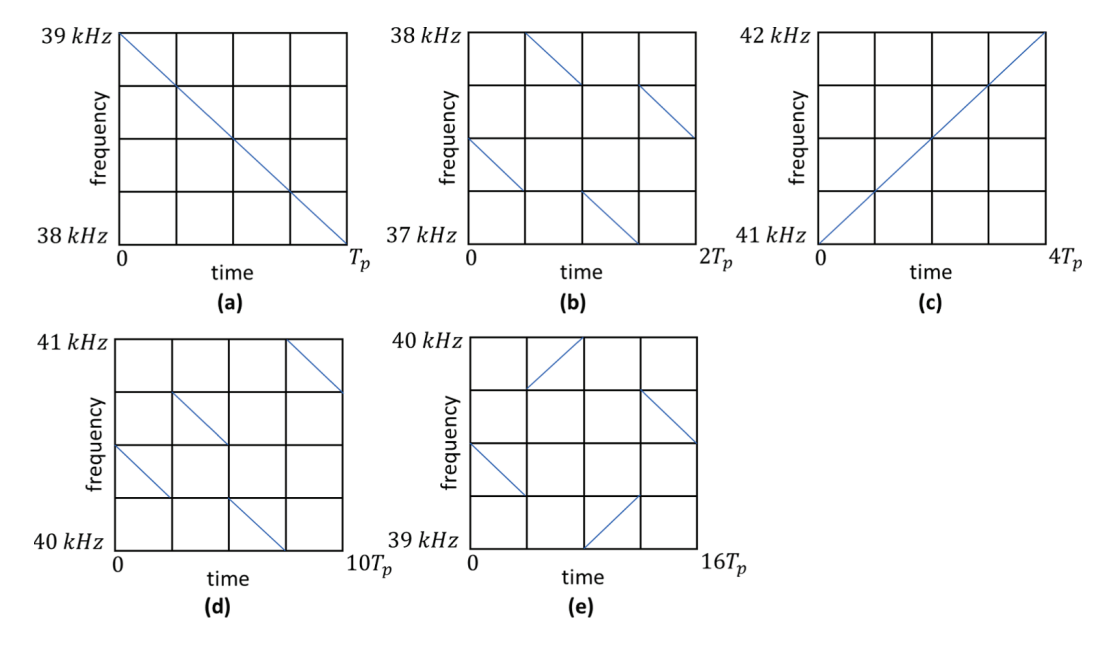


Fig. 8. Illustration of the preamble signals.

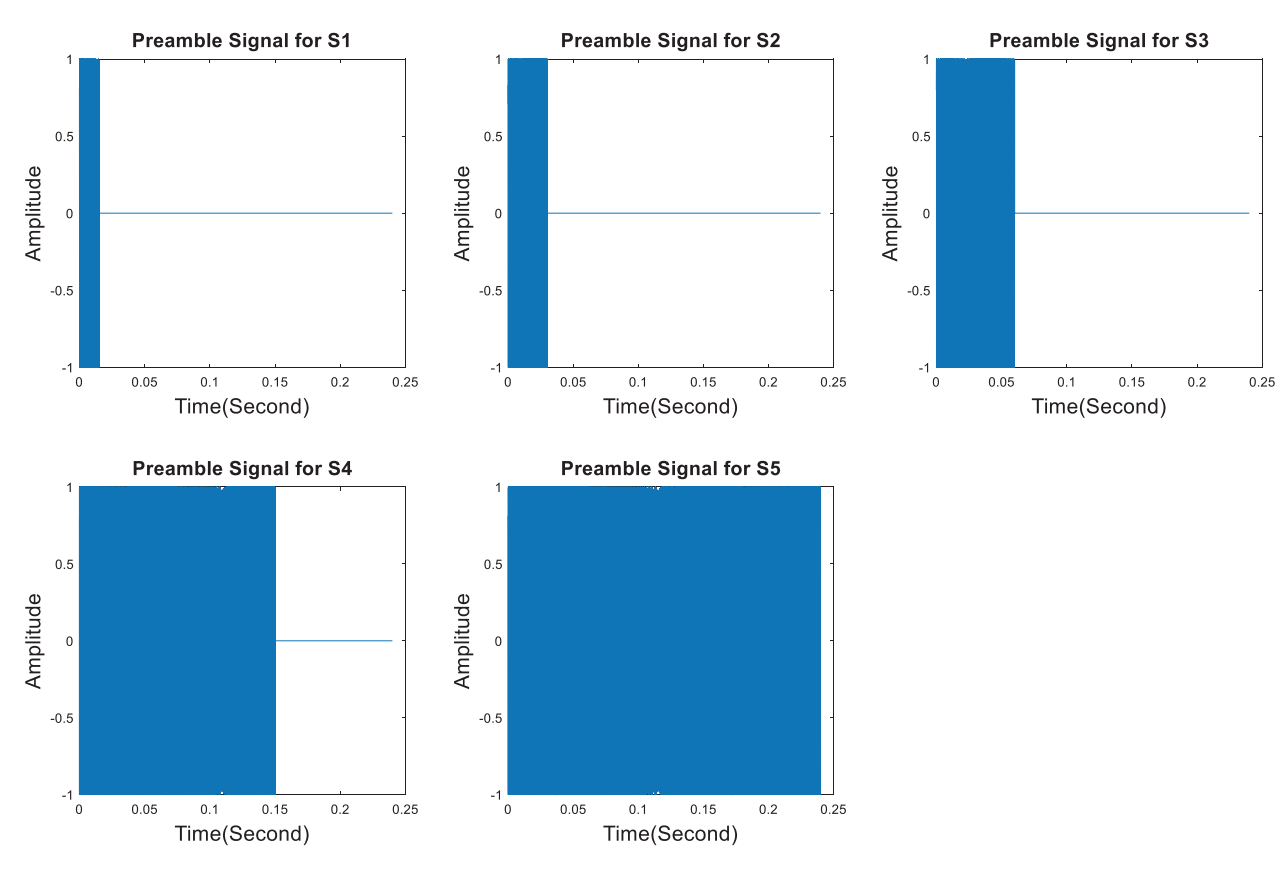


Fig. 9. Illustration of preamble waveforms.

A chirp signal sweeping from 10 kHz to 100 kHz (shown in Fig. 4.) is utilized to estimate the frequency channel responses. The received waveforms at different sensors are shown in Fig. 5. By use of PSD analysis as mentioned before, the PSD of received signals and the channel responses are illustrated in Fig. 6. The channels present frequency selectivity as the results show. The frequency response curves reach the peak around 40 kHz and drop approximately 40 dB per decade. The frequency responses indicate appropriate communication bandwidths for stress wave data transmission over each channel. Moreover, the impulse responses are presented in Fig. 7. based on 'CLEAN' algorithm, which provide access to channel characteristics in the perspective of time domain. The impulse responses are quite different among channels, thus it is extremely difficult to conduct equalization among SW channels, which explains

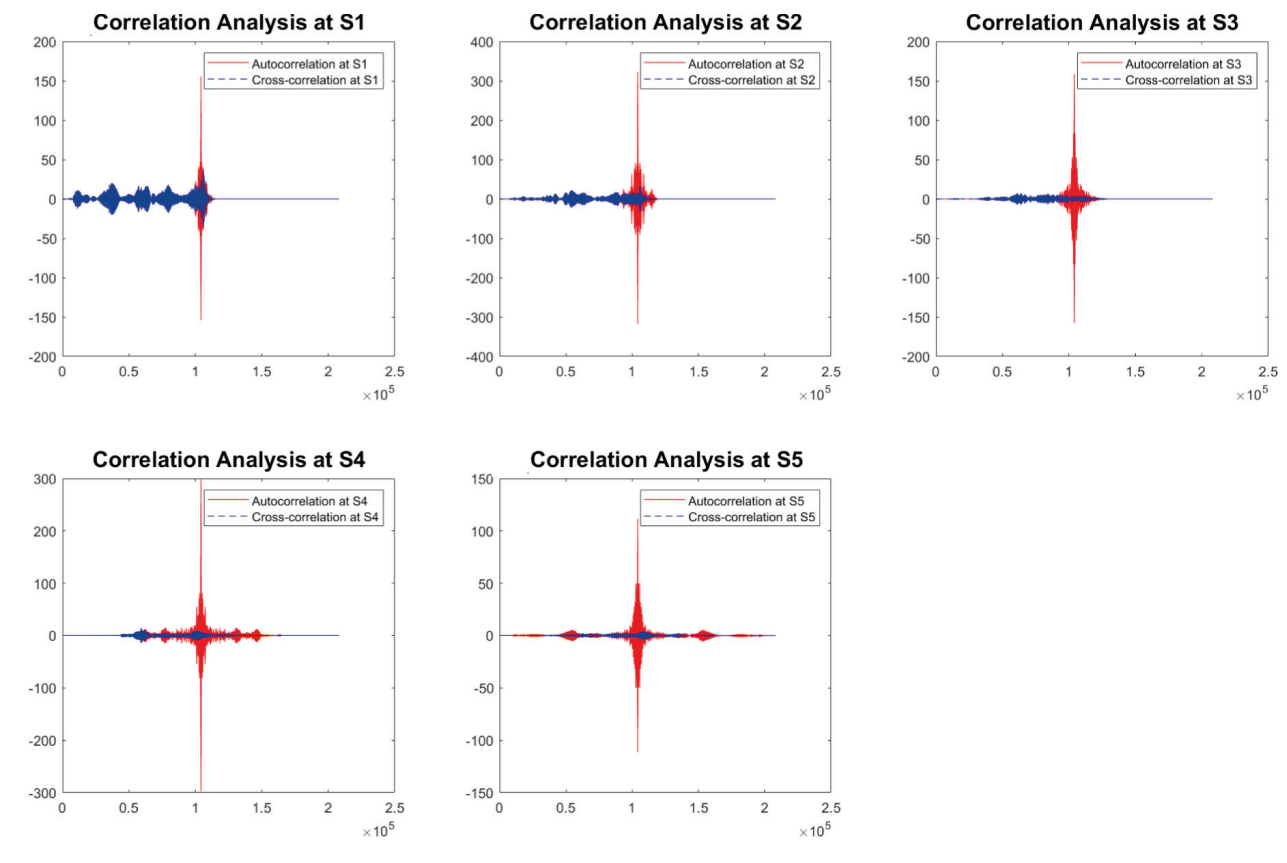


Fig. 10. Simulated correlation analysis.

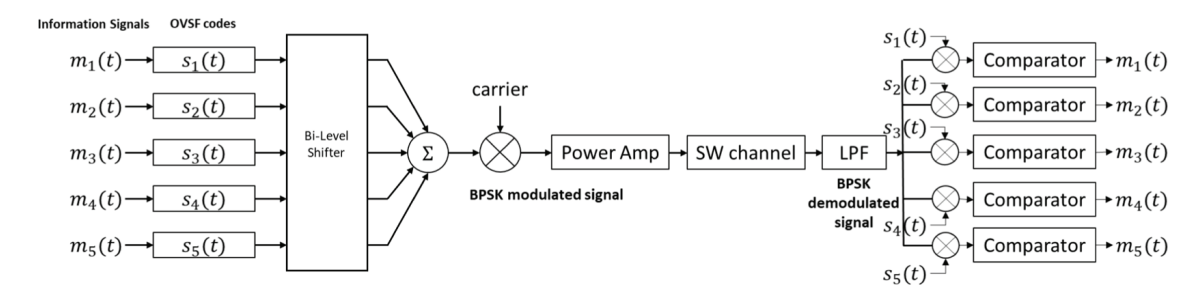


Fig. 11. Implementation of SW SIMO communication.

the reason that TDMA is applied to avoid inter-channel interferences. The impulse responses are then employed to simulate output signals in the follows.

3.2. Preamble signals design

As explained in Section 2, the preamble signals for each channel are designed based on OFDM chirp bases. The preamble signals are diversified by modifying the matrices utilized to multiply with the bases. The total time durations and bandwidths for each channel are varied to combat highly attenuative channels and suppress cross correlation interferences. Fig. 8. illustrates the preamble signals design and the corresponding waveforms are shown in Fig. 9. The first preamble signal occupies the shortest total time duration $T_p = 0.015$ s and every preamble signal has a bandwidth of 1 kHz.

Simulations of the correlation analysis are provided in Fig. 10. The output preamble waveforms are generated by convolving the proposed preamble waveforms with impulse responses of channels shown in Fig. 7. Then, the correlation analyses are conducted between the local preamble signal and the received waveforms. As shown in Fig. 10, red lines represent autocorrelation at different sensors while blue dashed lines stand for cross correlation with other received waveforms. The correlation results verify that the proposed preamble signals have good correlation properties under the effect of SW channels.

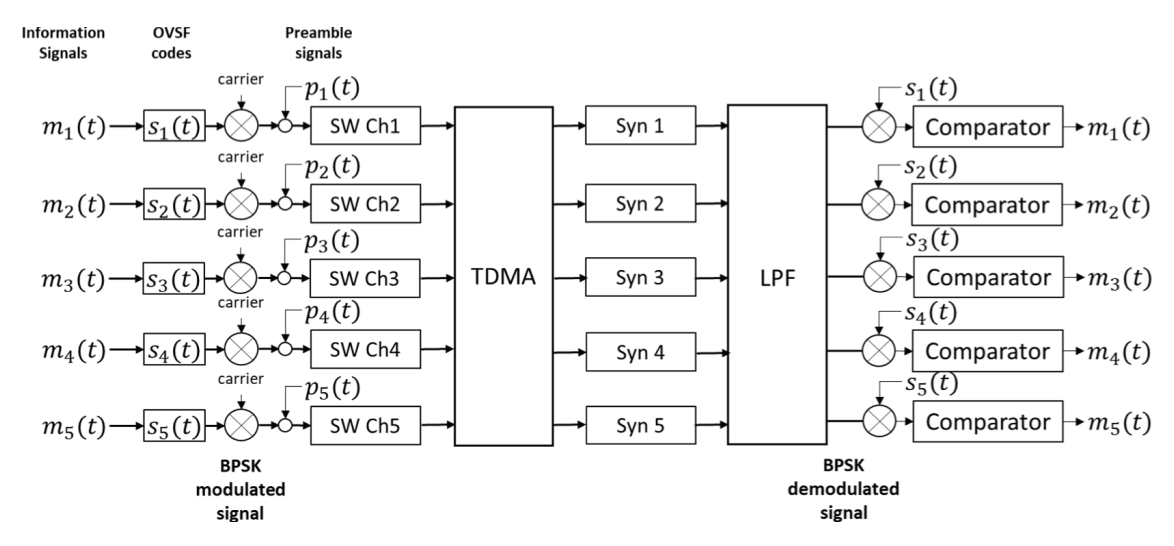


Fig. 12. Implementation of SW MISO communication.

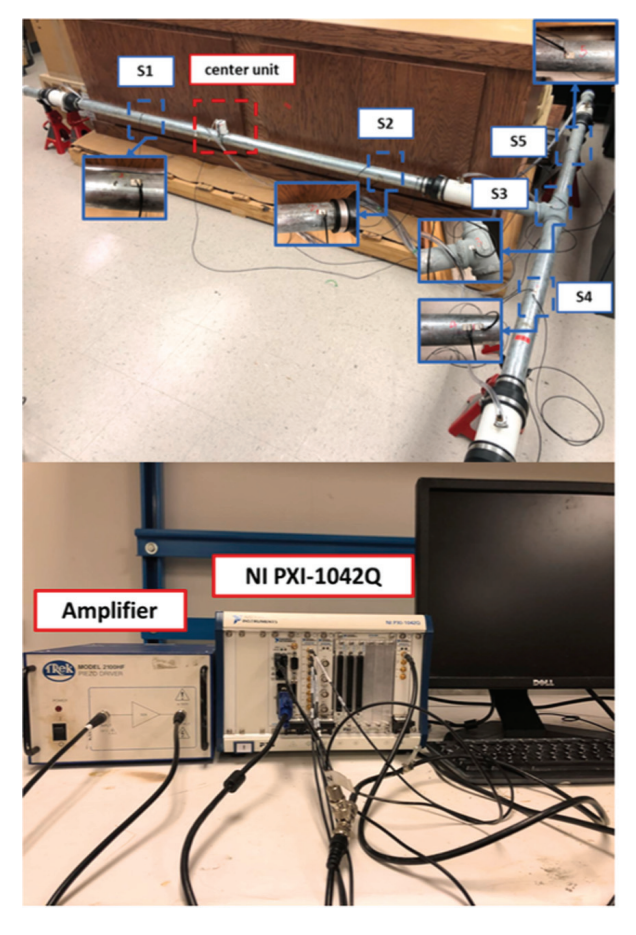


Fig. 13. Experimental setup.

3.3. Implementation of stress wave networking communication

As described in Section 2, the proposed stress wave networking communication system is achieved by exploiting different data transmission schemes for SIMO system and MISO system. In the SIMO data transmission system, shown in Fig. 11, information is encoded with OVSF codes and then modulated with binary shift keying (BPSK). It is worthwhile to mention that Hamming error-correcting codes are also utilized to minimize possible inter-symbol errors. The OVSF codes used in the system have a spreading factor (SF) of 16, which means every single code in the information is expanded by 16 chips. And the carrier wave (40 kHz) modulates

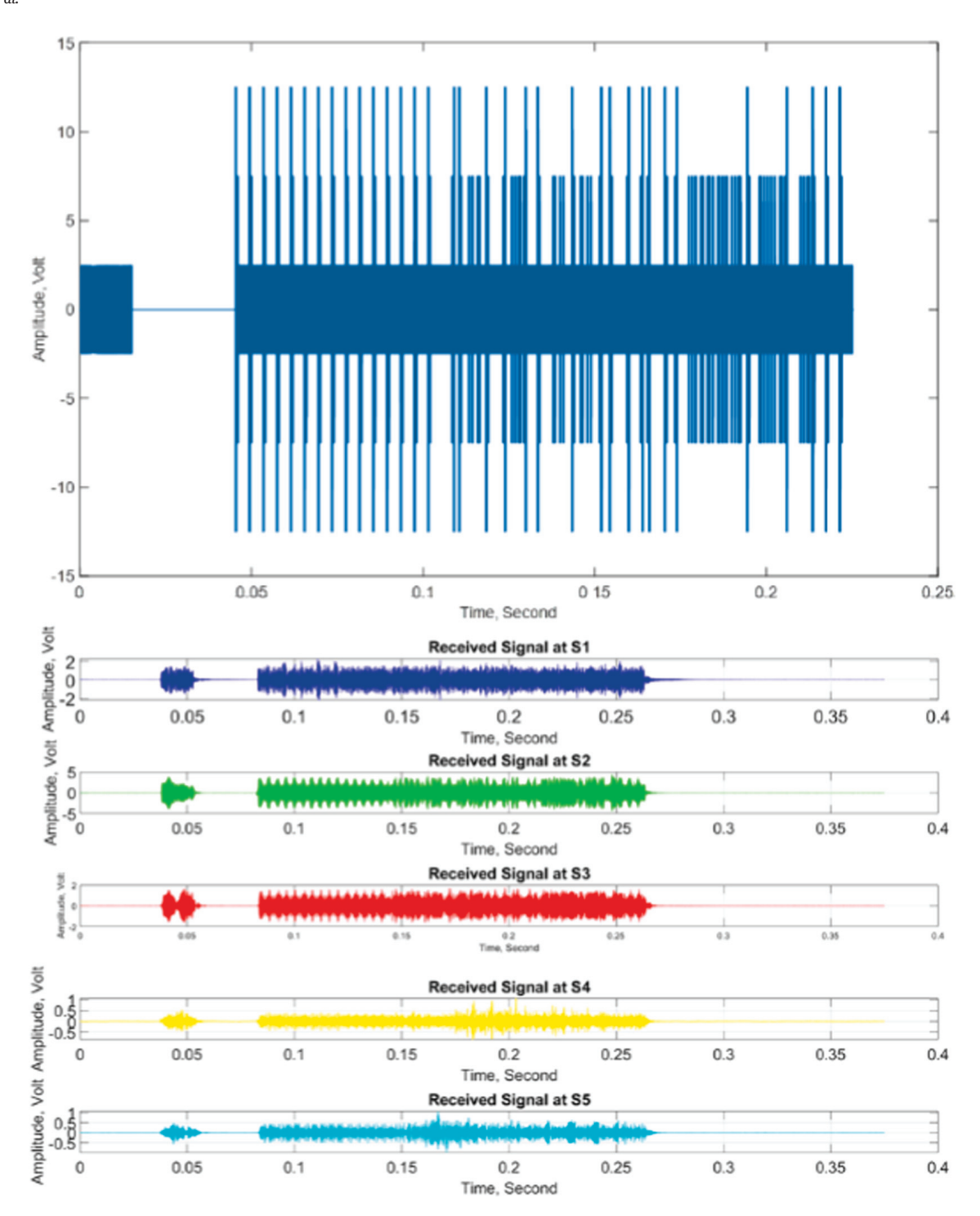


Fig. 14. The transmitting signal and received signals in the SW SIMO system. Top: the transmitting signal from the center unit; bottom: the received signals at multiple sensors.

the information with a data rate of 250 bps. Information bearing stress waves are received at different sensors after traveling through the pipeline, and demodulation of the received waveforms is subsequently carried out. Then, local OVSF codes are deployed to decode the information that is intended for each receiver. In the MISO data transmission system (Fig. 12), multiple sensors encode and modulate information into stress waves with a preamble signal in front, and the signals are launched in exclusive time segments. The center unit working as the unique receiver in the MISO system uses preamble signals to identify and synchronize each signal and then the received waveforms can be proceeded to be demodulated and decoded.

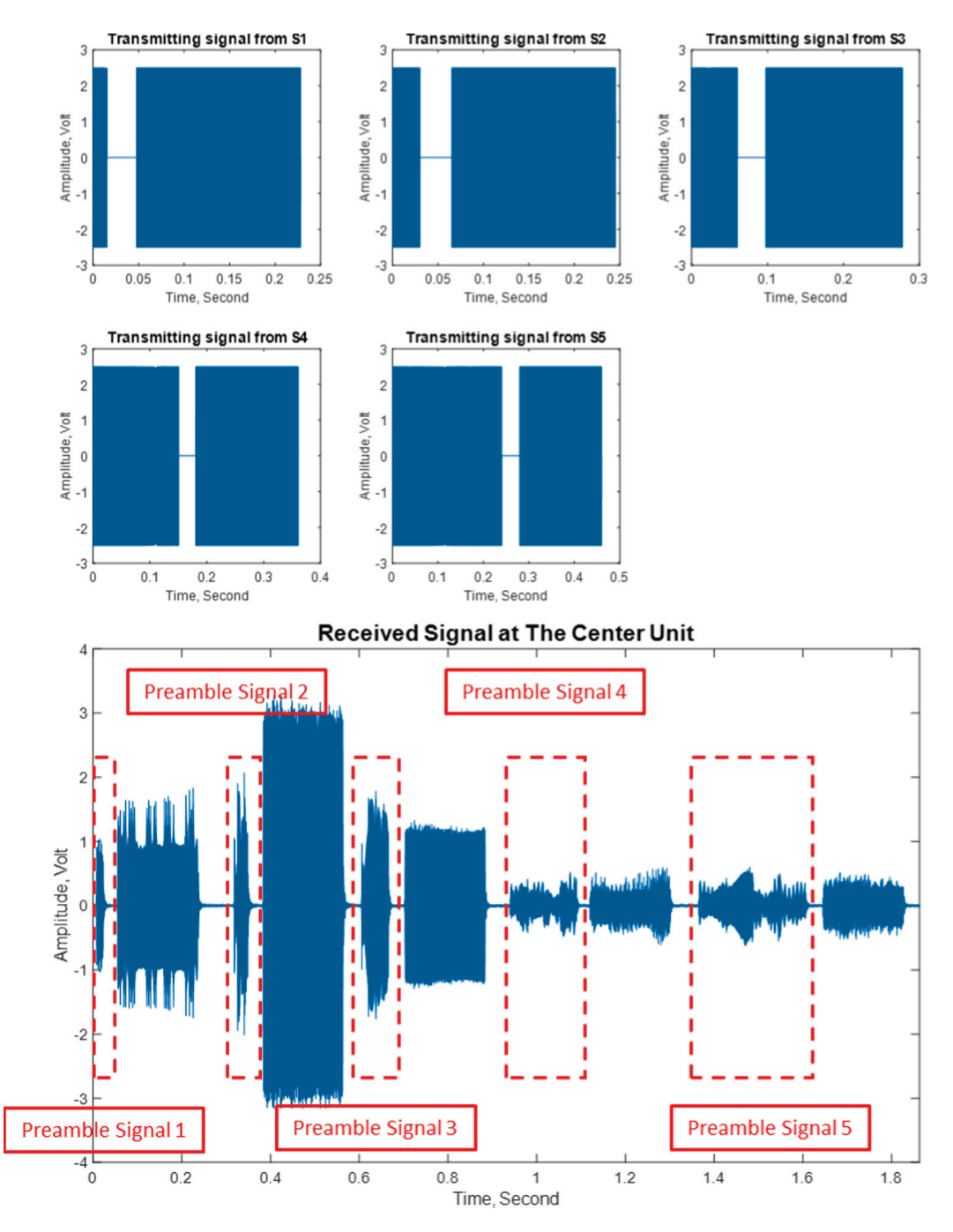


Fig. 15. The transmitting signals and received signal in the SW MISO system. Top: the transmitting signals from S1 to S5; bottom: the received signal at the center unit.

4. Experiment and analysis

Experiments are conducted on a T-shape pipeline to verify the performances of the proposed method. Two galvanized steel pipes $(53.8 \times 50.8 \times 3048 \text{mm})$ are welded in the configuration, as shown in Fig. 13. A piezoelectric transducer is clamped on the pipe to work as the center unit, and five piezoelectric plates are mounted at different locations. As presented in Fig. 13, a National Instrument PXI-1042Q is employed as the digital-to-analog device as well as the data acquisition system. The sampling frequency is set to be 400 kHz to meet the requirement of signal recovery.

The testing is carried out in the lab environment. In the SIMO system, the center unit launches signals simultaneously and the received signals at different sensors are presented in Fig. 14. As shown in the figure, original waveforms are distorted and elongated by the stress wave channels with traveling distances. Waveforms received at Sensor 4 and Sensor 5 attenuate more due to the longest distance and the welding connection. All the received signals can be correctly decoded using local OVSF codes at different sensors. In the MISO system, signals from different sensors are recorded respectively and arranged in a proper order, as shown in Fig. 15. Received

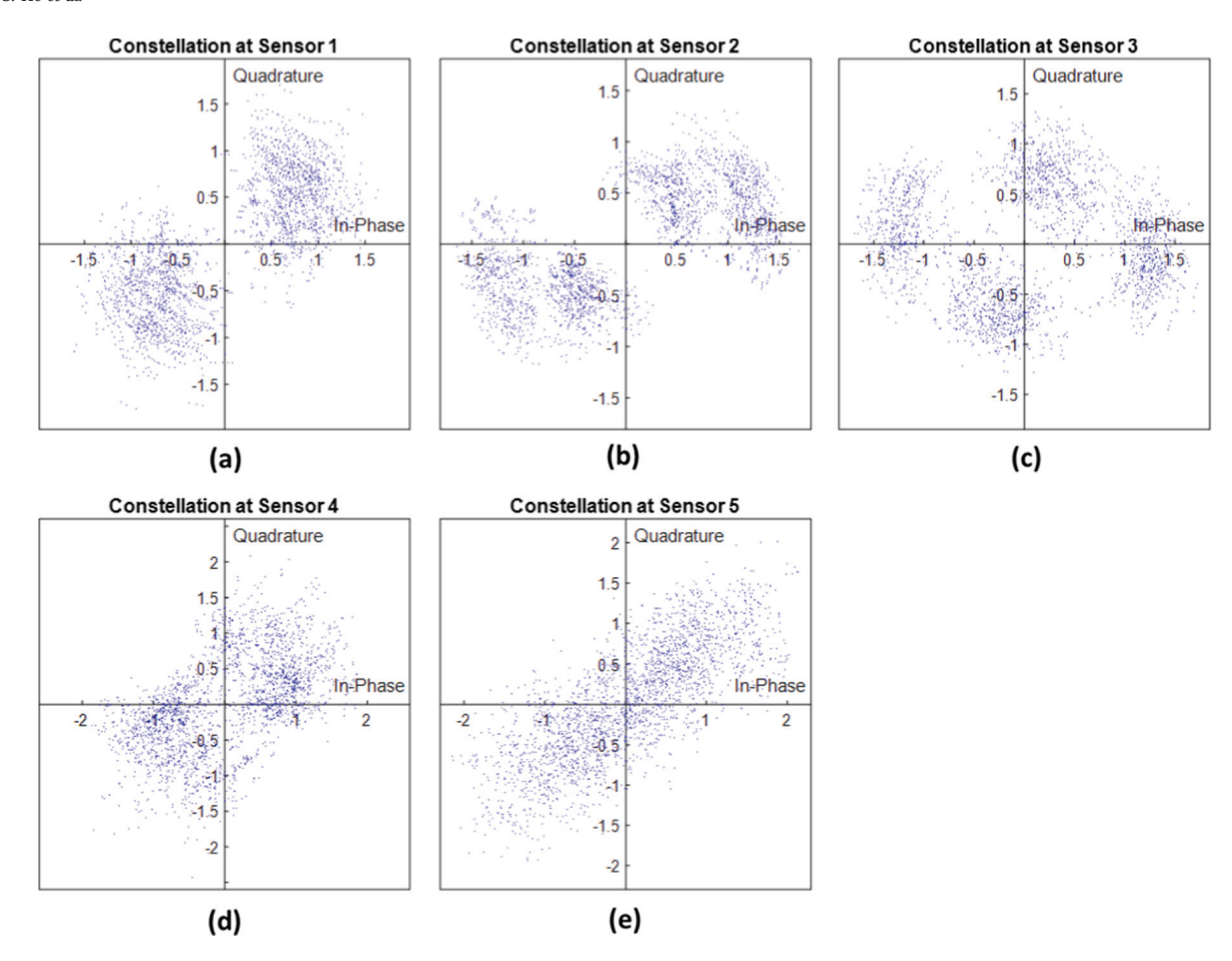


Fig. 16. Constellation diagram for experimental results. Diagrams from (a) to (e) represent experimental constellation diagrams of S1 to S5.

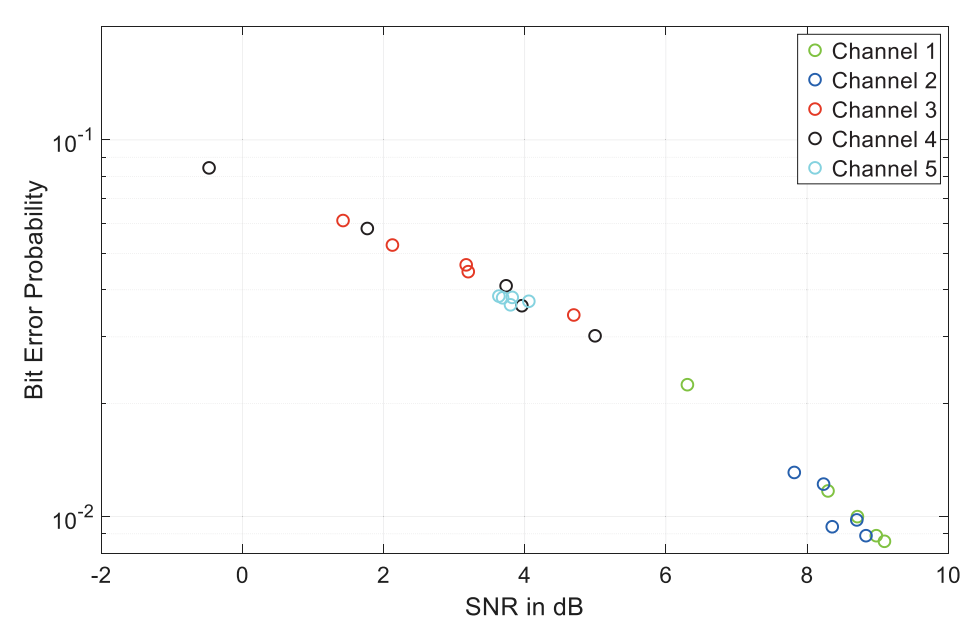


Fig. 17. The BER estimation.

signals display different amplitudes and distortion due to different channel effects. The preamble signals can accurately synchronize the arrival time of each signal because of the good correlation performance. Then signals from multiple sensors can be interpreted at the center unit.

The constellation diagrams, as shown in Fig. 16, are depicted based on the experimental results. Since binary phase shift keying (BPSK), which is employed in our method as the modulation scheme, is the simplest form of phase shift keying (PSK), and the carrier phases shift between 0° and 180° . Points located at (1,0) and (-1,0) in the constellation diagram hence represent the corresponding phases. Therefore, the scatter points that are more concentrated around (1,0) and (-1,0) indicate better communication performances. As shown in Fig. 16, the received signals at S1 and S2 perform best in signal recovery, while the last two figures show more potential ambiguity. The results are in accordance with the received amplitudes shown in Fig. 17. The bit error rate (BER) estimation based on Monte Carlo simulation also supports the same results that received signals of a closer distance possess higher signal-to-noise ratio (SNR). Additionally, welding connections and other joints on the pipeline may influence long-distance networking stress wave communication because stress waves are reduced when propagating through the joints.

5. Conclusion and future work

A stress wave networking communication method is developed in this paper. Based on the characteristics of stress wave propagation along pipelines, we employ different data transmission schemes for the single-input-multiple-output (SIMO) system and multiple-input-single-output (MISO) system. In the SIMO system, orthogonal variable spreading factor (OVSF) codes are introduced to enable multiple signals to be transmitted simultaneously. The orthogonality among OVSF codes ensures the received signals at different sensors can be correctly decoded using local OVSF codes. Time division multiple access (TDMA) is applied in the MISO system. Different sensors occupy exclusive time segments to emit signals to the center unit. The design of preamble signals enables the center unit to accurately measure the arrival time of every signal. Binary shift keying (BPSK) is adopted in this paper to modulate encoded signals. The proposed method is implemented on a T-shape pipeline structure which is welded by two pipeline components in the laboratory environment. The experimental results verified that the communication data rate among sensors can achieve 250 bps with the spreading factor (SF) equal to 16. Therefore, the proposed method is believed to be feasible and promising for data transmission among sensor networks, especially for those difficult to deploy conventional communications.

In the procedure of implementing the method on pipelines, we also found limitations of the proposed method. The future works should be devoted to improving the method developed in this paper. Firstly, the available bandwidth is found to be narrow based on the channel estimation. The reasons may come from the structure of the pipelines or the transducers used in the experiments, thus only a single carrier is utilized to deliver information. It is worthwhile to explore the method to broaden available bandwidth in stress wave communication, so that multiple carriers can be employed to transmit information in parallel and the communication performances can be hence significantly improved. Secondly, since different channels have quite distinct impulse responses, equalization between stress wave channels is not investigated in this paper. In future works, explorations on equalizing stress wave channels will help a variety of data transmission schemes to be achieved in stress wave communication systems and will certainly enhance communication performances. Last but not the least, the experiments were conducted only on a small-scale pipeline structure, which is of much simplicity compared to real pipelines in the field. Testing will be conducted on more complex pipeline structures in the future and corresponding technical improvements are needed for different conditions.

Declaration of Competing Interest

The authors declare that they have no known competing financial interests or personal relationships that could have appeared to influence the work reported in this paper.

Acknowledgements

This research was partially supported by Texas Commission on Environmental Quality through Subsea Systems Institute Award #582-15-57593 and National Science Foundation (NSF) grant No. 1801925. This project was paid for [in part] with federal funding from the Department of the Treasury through the State of Texas under the Resources and Ecosystems Sustainability, Tourist Opportunities, and Revived Economies of the Gulf Coast States Act of 2012 (RESTORE Act).

The content, statements, findings, opinions, conclusions, and recommendations are those of the author(s) and do not necessarily reflect the views of the State of Texas or the Treasury or the NSF.

Conflict of Interests

Potential Conflict of Interests: Dr. Gangbing Song holds financial interest in AEM which is a startup company in structural health monitoring.

References

[1] F. Wang, Z. Chen, G. Song, Monitoring of multi-bolt connection looseness using entropy-based active sensing and genetic algorithm-based least square support vector machine, Mechanical Systems and Signal Processing 136 (2020), 106507.

- [2] M. Mitra, S. Gopalakrishnan, Guided wave based structural health monitoring: A review, Smart Materials and Structures 25 (5) (2016) 053001, https://doi.org/10.1088/0964-1726/25/5/053001.
- [3] G. Lu, T. Wang, M. Zhou, Y. Li, Characterization of Ultrasonic Energy Diffusion in a Steel Alloy Sample with Tensile Force Using PZT Transducers, Sensors 19 (2019) 2185.
- [4] Q. Kong, R.H. Robert, P. Silva, Y. Mo, Cyclic crack monitoring of a reinforced concrete column under simulated pseudo-dynamic loading using piezoceramic based smart aggregates, Applied sciences 6 (2016) 341.
- [5] T. Wandowski, P. Malinowski, W. Ostachowicz, Circular sensing networks for guided waves based structural health monitoring, Mechanical Systems and Signal Processing 66 (2016) 248–267.
- [6] M. Ho, S. El-Borgi, D. Patil, G. Song, Inspection and monitoring systems subsea pipelines: A review paper, Structural Health Monitoring 19 (2) (2020) 606-645.
- [7] M. Eybpoosh, M. Berges, H.Y. Noh, An energy-based sparse representation of ultrasonic guided-waves for online damage detection of pipelines under varying environmental and operational conditions, Mechanical Systems and Signal Processing 82 (2017) 260–278.
- [8] G. Du, Q. Kong, F. Wu, J. Ruan, G. Song, An experimental feasibility study of pipeline corrosion pit detection using a piezoceramic time reversal mirror, Smart Materials and Structures 25 (2016), 037002.
- [9] V. Marcantonio, D. Monarca, A. Colantoni, M. Cecchini, Ultrasonic waves for materials evaluation in fatigue, thermal and corrosion damage: A review, Mechanical Systems and Signal Processing 120 (2019) 32–42.
- [10] J. Zhu, L. Ren, S.-C. Ho, Z. Jia, G. Song, Gas pipeline leakage detection based on PZT sensors, Smart Materials and Structures 26 (2017), 025022.
- [11] G. Du, L. Huo, Q. Kong, G. Song, Damage detection of pipeline multiple cracks using piezoceramic transducers, Journal of Vibroengineering 18 (2016) 2828–2838.
- [12] L. Satyarnarayan, J. Chandrasekaran, B. Maxfield, K. Balasubramaniam, Circumferential higher order guided wave modes for the detection and sizing of cracks and pinholes in pipe support regions, NDT & E International 41 (2008) 32–43.
- [13] J. Zhu, S.C.M. Ho, D. Patil, N. Wang, R. Hirsch, G. Song, Underwater pipeline impact localization using piezoceramic transducers, Smart Materials and Structures 26 (2017), 107002.
- [14] Y. Liu, M. Zhang, X. Yin, Z. Huang, L. Wang, Debonding detection of reinforced concrete (RC) beam with near-surface mounted (NSM) pre-stressed carbon fiber reinforced polymer (CFRP) plates using embedded piezoceramic smart aggregates (SAs), Applied Sciences 10 (2020) 50.
- [15] J. Jiang, S.C.M. Ho, T. Tippitt, Z. Chen, G. Song, Feasibility study of a touch-enabled active sensing approach to inspecting subsea bolted connections using piezoceramic transducers, Smart Materials and Structures 29 (8) (2020) 085038, https://doi.org/10.1088/1361-665X/ab84ba.
- [16] F. Wang, S.C.M. Ho, L. Huo, G. Song, A novel fractal contact-electromechanical impedance model for quantitative monitoring of bolted joint looseness, Ieee Access 6 (2018) 40212–40220.
- [17] N. Li, F. Wang, G. Song, New entropy-based vibro-acoustic modulation method for metal fatigue crack detection: An exploratory study, Measurement 150 (2020) 107075, https://doi.org/10.1016/j.measurement.2019.107075.
- [18] F. Wang, G. Song, Bolt early looseness monitoring using modified vibro-acoustic modulation by time-reversal, Mechanical Systems and Signal Processing 130 (2019) 349–360.
- [19] Y. Jin, A. Eydgahi, Monitoring of distributed pipeline systems by wireless sensor networks, Proceedings of The (2008) 213-222.
- [20] Y. Xu, M. Luo, Q. Liu, G. Du, G. Song, PZT transducer array enabled pipeline defect locating based on time-reversal method and matching pursuit de-noising, Smart Materials and Structures 28 (7) (2019) 075019, https://doi.org/10.1088/1361-665X/ab1cc9.
- [21] B. Chen, C. Hei, M. Luo, M.S.C. Ho, G. Song, Pipeline two-dimensional impact location determination using time of arrival with instant phase (TOAIP) with piezoceramic transducer array, Smart Materials and Structures 27 (10) (2018) 105003, https://doi.org/10.1088/1361-665X/aadaa9.
- [22] S. Siu, Q. Ji, W. Wu, G. Song, Zhi Ding, Stress wave communication in concrete: I Characterization of a smart aggregate based concrete channel, Smart Materials and Structures 23 (12) (2014) 125030, https://doi.org/10.1088/0964-1726/23/12/125030.
- [23] S. Siu, J.i. Qing, K. Wang, G. Song, Z. Ding, Stress wave communication in concrete: II Evaluation of low voltage concrete stress wave communications utilizing spectrally efficient modulation schemes with PZT transducers, Smart Materials and Structures 23 (12) (2014) 125031, https://doi.org/10.1088/0964-1726/23/12/125031.
- [24] Q. Ji, M. Ho, R. Zheng, Z. Ding, G. Song, An exploratory study of stress wave communication in concrete structures, Smart Structures and Systems 15 (1) (2015) 135–150.
- [25] Q. Ji, Z. Ding, N. Wang, M. Pan, G. Song, A Novel Waveform Optimization Scheme for Piezoelectric Sensors Wire-Free Charging in the Tightly Insulated Environment, IEEE Internet of Things Journal 5 (3) (2018) 1936–1946.
- [26] T.L. Murphy. Ultrasonic digital communication system for a steel wall multipath channel: Methods and results. Knolls Atomic Power Laboratory (KAPL). Niskayuna, NY (United States). 2005.
- [27] G. Saulnier, H. Scarton, A. Gavens, D. Shoudy, T. Murphy, M. Wetzel, S. Bard, S. Roa-Prada, P. Das. P1g-4 through-wall communication of low-rate digital data using ultrasound, Ultrasonics Symposium, 2006. IEEE, IEEE. 2006. 1385-1389.
- [28] M. Bielinski, K. Wanuga, R. Primerano, M. Kam, K.R. Dandekar, Application of adaptive OFDM bit loading for high data rate through-metal communication, 2011 IEEE Global Telecommunications Conference-GLOBECOM 2011, IEEE (2011) 1–5.
- [29] K. Wanuga, M. Bielinski, R. Primerano, M. Kam, K.R. Dandekar. High-data-rate ultrasonic through-metal communication. IEEE transactions on ultrasonics, ferroelectrics, and frequency control. 59. 2012. 2051-2053.
- [30] Ding-Xin Yang, Zheng Hu, Hong Zhao, Hai-Feng Hu, Yun-Zhe Sun, Bao-Jian Hou, Through-metal-wall power delivery and data transmission for enclosed sensors: A review, Sensors 15 (12) (2015) 31581–31605.
- [31] K. Manolakis, U. Krüger, K. Krüger, M. Gutierrez-Estevez, S. Mikulla, V. Jungnickel. Borehole communication with acoustic ofdm, Int. OFDM-Workshop (InOWo'11), 2011.
- [32] M.A. Gutierrez-Estevez, U. Krüger, K.A. Krueger, K. Manolakis, V. Jungnickel, K. Jaksch, K. Krueger, S. Mikulla, R. Giese, M. Sohmer. Acoustic broadband communications over deep drill strings using adaptive OFDM, Wireless Communications and Networking Conference (WCNC). 2013. IEEE, IEEE. 2013. 4089-4094.
- [33] A. Wu, S. He, Y. Ren, N. Wang, S.C.M. Ho, G. Song, Design of a new stress wave-based pulse position modulation (PPM) communication system with piezoceramic transducers, Sensors 19 (2019) 558.
- [34] Y. Jin, Y. Ying, D. Zhao, in: Time reversal data communications on pipes using guided elastic waves: Part II. Experimental studies, International Society for Optics and Photonics, 2011, p. 79840C.
- [35] Yuanwei Jin, Yujie Ying, Deshuang Zhao, Data communications using guided elastic waves by time reversal pulse position modulation: Experimental study, Sensors 13 (7) (2013) 8352–8376.
- [36] Y. Jin, D. Zhao, Y. Ying, Time reversal data communication on pipes using guided elastic waves—part I: basic principles Proc, SPIE Health Monitoring of Structural and Biological Systems 7984 (2012) 1–12.
- [37] X. Huang, J. Saniie, S. Bakhtiari, A. Heifetz. Applying EMAT for ultrasonic communication through steel plates and pipes, 2018 IEEE International Conference on Electro/Information Technology (EIT). IEEE. 2018. 0379-0383.
- [38] S. Chakraborty, G.J. Saulnier, K.W. Wilt, R.B. Litman, H.A. Scarton. Low-rate ultrasonic communication axially along a cylindrical pipe, Ultrasonics Symposium (IUS), 2014 IEEE International, IEEE, 2014. 547-551.
- [39] S. Chakraborty, G.J. Saulnier, K.W. Wilt, E. Curt, H.A. Scarton, R.B. Litman. Low-power, low-rate ultrasonic communications system transmitting axially along a cylindrical pipe using transverse waves. IEEE transactions on ultrasonics, ferroelectrics, and frequency control. 62. 2015. 1788-1796.
- [40] K.M. Joseph, T. Watteyne, B. Kerkez, Awa: Using water distribution systems to transmit data, Transactions on Emerging Telecommunications Technologies 29 (2018), e3219.
- [41] P.T. Gough, A fast spectral estimation algorithm based on the FFT, IEEE transactions on signal processing 42 (1994) 1317–1322.
- [42] J. Hogbom, Aperture synthesis with non-rectangular distribution of interferometric baselines, Astron. Astrophys. Suppl. v15, 417-426.

- [43] R. Scholtz, R.-M. Cramer, M. Win, Evaluation of the propagation characteristics of ultra-wideband communication channels, IEEE Antennas and Propagation Society International Symposium. 1998 Digest. Antennas: Gateways to the Global Network. Held in conjunction with: USNC/URSI National Radio Science Meeting (Cat. No. 98CH36. IEEE. 1998. 626-630.
- [44] P. Welch, The use of fast Fourier transform for the estimation of power spectra: a method based on time averaging over short, modified periodograms, IEEE Transactions on Audio and Electroacoustics 15 (1967) 70–73.
- [45] W. Yang, Z. Naitong, A new multi-template CLEAN algorithm for UWB channel impulse response characterization, in: 2006 International Conference on Communication Technology, IEEE, 2006, pp. 1–4.
- [46] L. Feng, P. Fan, X. Tang, A general construction of OVSF codes with zero correlation zone, IEEE Signal Processing Letters 14 (2007) 908-911.
- [47] H. Li, Y. Zhao, Z. Cheng, D. Feng, OFDM chirp waveform diversity design with correlation interference suppression for MIMO radar, IEEE Geoscience and Remote Sensing Letters 14 (2017) 1032–1036.
- [48] M.O. Khyam, M. Noor-A-Rahim, X. Li, C. Ritz, Y.L. Guan, S.S. Ge, Design of chirp waveforms for multiple-access ultrasonic indoor positioning, IEEE Sensors Journal 18 (2018) 6375–6390.